

Generalization of the Tavis-Cummings model for multi-level anharmonic systems: insights on the second excitation manifold

J. Campos-Gonzalez-Angulo and J. Yuen-Zhou^{a)}

Department of Chemistry and Biochemistry, University of California San Diego, La Jolla, California 92093, USA

Confined electromagnetic modes strongly couple to collective excitations in ensembles of quantum emitters, producing light-matter hybrid states known as polaritons. Under such conditions, the discrete multilevel spectrum of molecular systems offers an appealing playground for exploring multiphoton processes. This work contrasts predictions from the Tavis-Cummings (TC) model, in which the material is a collection of two-level systems, with the implications of considering additional energy levels with harmonic and anharmonic structures. We discuss the exact eigenspectrum, up to the second excitation manifold, of an arbitrary number N of oscillators collectively coupled to a single cavity mode in the rotating-wave approximation. Elaborating on our group-theoretic approach [*New J. Phys.* 23, 063081 (2021)], we simplify the brute-force diagonalization of a gigantic $N^2 \times N^2$ Hamiltonian (where $N = 10^6 - 10^{10}$, as experiments suggest) to the diagonalization of, at most, 4×4 matrices. We thoroughly discuss the eigenstates and the consequences of weak and strong anharmonicities. Furthermore, we find resonant conditions between bipolaritons and anharmonic transitions where two-photon absorption can be enhanced. Finally, we conclude that energy shifts in the polaritonic states induced by anharmonicities become negligible for large N . Thus, calculations with a single or few emitters qualitatively fail to represent the nonlinear optical response of the collective strong coupling regime. Our work highlights the rich physics of multilevel anharmonic systems coupled to cavities absent in standard models of quantum optics. We also provide concise tabulated expressions for eigenfrequencies and transition amplitudes, which should serve as a reference for future spectroscopic studies of molecular polaritons.

I. INTRODUCTION

The strong coupling (SC) of confined photonic modes and excitations in semiconductors and molecular materials leads to a wealth of interesting chemical and condensed-matter physics phenomena¹⁻⁵ such as room-temperature Bose-Einstein condensation,⁶⁻⁹ long-range energy transfer,^{10,11} modification of chemical reactivity,¹²⁻¹⁴ and quantum information processing.^{15,16} Strong coupling leads to hybrid light-matter quantum modes known as polaritons, originally characterized for electronic excitations in bulk materials,^{17,18} and later on studied in cavity systems.^{19,20} Within linear response, the formalism to understand these systems is naturally based on a harmonic approximation for the material degrees of freedom.¹⁸ However, to understand nonlinear optical properties, the material degrees of freedom are typically modeled as two-level quantum emitters, leading to the very well-studied Jaynes-Cummings and Rabi models in the case of a single emitter,^{21,22} or the Tavis-Cummings (TC) and Dicke models in the collective regime.^{23,24} Recently, there has been an increasing interest in the properties of vibrational polariton systems resulting from the strong coupling of infrared (IR) cavity modes and ensembles of localized high-frequency vibrational modes in molecules in condensed phases.²⁵⁻³² The multilevel anharmonic spectrum of these vibrational modes implies that their accurate description should invoke more than two levels per emitter. Indeed, consideration of more realistic vibrational SC systems involving anharmonicities has been the subject of theoretical explorations, such as the use of single-molecule models to explain cavity-induced modifications to chemical reactivity,³³⁻³⁷ as well as the use of many-molecule models

to explain non-linear response experiments.^{28,38-43} In particular, recent work⁴⁴⁻⁴⁹ has elucidated novel multiphoton absorption phenomena where the TC description is insufficient, and a multilevel anharmonic spectrum of the material is essential. These effects go beyond vibrational SC and should have analogues in other electromagnetic ranges, such as those systems under electronic SC where more than two electronic states per quantum emitter must be considered.

While theoretical complexities emerging from the multilevel anharmonic spectrum of the oscillators are expected, they can be overcome by taking advantage of the permutational symmetries derived from the assumption that the emitters behave identically.⁵⁰⁻⁵³ For regimes in which the counterrotating (non-energy conserving) terms of the coupling can be disregarded, the Hamiltonian can be separated according to the total number of excitations allocated in the many-body states that conform the basis of the Hilbert space.^{54,55} The general strategy to simplify and solve the Schrödinger equation for this instance can be found in ref. 56, work on which the present manuscript elaborates by describing in detail the wavefunctions and the energy spectrum resulting from diagonalizing the Hamiltonian of a collection of anharmonic multilevel quantum emitters dipolarly coupled to a single cavity mode. In particular, we focus on the structure of the subspace built from states bearing two excitations and compare it with the well-known solutions of the first excitation manifold. For systems under collective SC, the number of emitters is very large at $N \approx 10^6 - 10^{10}$, and a brute-force numerical diagonalization to solve for the eigenspectrum of these hybrid light-matter systems is unattainable. Our method exploiting the permutational symmetry arising from the consideration of N identical emitters dramatically reduces the problem to the diagonalization of very small matrices.

The organization of this manuscript is as follows: in sec-

^{a)}Electronic mail: joelyuen@ucsd.edu; http://yuenzhougroup.ucsd.edu

tion II we revisit the first-excitation manifold and present the tools and vocabulary of polaritonic states that permeate the remaining of the paper. Section III opens by introducing generalities of the states with two excitations and proceeds with the presentation of the eigenstates for the TC model. These solutions are contrasted with those obtained after including an additional energy level per emitter, in the harmonic and anharmonic regimes, respectively. Tabulated expressions are also provided so that this work serves as a future reference for work on molecular polariton spectroscopy. Finally, the conclusions are presented in section IV.

II. THE FIRST EXCITATION MANIFOLD

For a collection of N identical multi-level quantum emitters interacting with a confined electromagnetic mode of frequency ω_0 in the regime where the rotating-wave approximation is valid, the total number of excitations in the system, n_{exc} , is a conserved quantity that defines the so-called excitation manifolds.

When $n_{\text{exc}} = 0$, all the components of the ensemble are in their respective ground states, and the system is characterized by the $(N + 1)$ -body state $|0\rangle$.

A basis can be defined for states with $n_{\text{exc}} = 1$, such that the excitation is localized on each of the emitters. To be specific, we have

$$|1_0\rangle = \hat{a}_0^\dagger |0\rangle, \quad (1a)$$

and

$$|1_{i>0}\rangle = \left(\hat{\sigma}_i^{(0)}\right)^\dagger |0\rangle, \quad (1b)$$

where \hat{a}_0^\dagger is the creation operator acting on the EM mode, and $\hat{\sigma}_i^{(v)}$ is the local operator acting on the i th emitter projecting the state $|v + 1\rangle$ onto $|v\rangle$. The notation in eq. (1) implies that all particles not explicitly indicated are in their respective ground states.

The Hamiltonian \hat{H}_1 describes the system in the singly excited manifold. In the basis defined in eq. (1), the matrix elements of \hat{H}_1 , in units of \hbar , are given by

$$\langle 1_i | \hat{H}_1 | 1_j \rangle = \begin{cases} \omega_0 & \text{if } i = j = 0 \\ \omega_{10} & \text{if } i = j > 0 \\ g_{01} & \text{for } i = 0, j > 0, \\ g_{10} & \text{for } i > 0, j = 0 \\ 0 & \text{otherwise} \end{cases} \quad (2)$$

where ω_{uv} is the excitation frequency between molecular energy levels u and v , and $g_{uv} = \sqrt{\frac{\omega_{uv}}{2\hbar\epsilon_0\mathcal{V}}} \langle u | \hat{\mu} | v \rangle$ is a coupling constant with \mathcal{V} the mode volume, and $\hat{\mu}$ the transition dipole moment operator (\hbar is the reduced Planck's constant, and ϵ_0 is the permittivity of the vacuum).

The system remains unchanged upon permutations of the emitters; therefore, its description can be simplified using the

SU(2) collective operators^{57,58}

$$\hat{f}_-^{(v)} = \sum_{i=1}^N \hat{\sigma}_i^{(v)}, \quad (3a)$$

$$\hat{f}_+^{(v)} = \left(\hat{f}_-^{(v)}\right)^\dagger, \quad (3b)$$

and

$$\hat{f}_0^{(v)} = \frac{1}{2} \left[\hat{f}_+^{(v)}, \hat{f}_-^{(v)} \right], \quad (3c)$$

which adhere to the angular momentum algebra, i.e.,

$$\left[\hat{f}_0^{(v)}, \hat{f}_\pm^{(v)} \right] = \hat{f}_\pm^{(v)}, \quad (4a)$$

$$\left[\hat{f}_+^{(v)}, \hat{f}_-^{(v)} \right] = 2\hat{f}_0^{(v)}. \quad (4b)$$

Since these operators are permutationally invariant, they carry the totally-symmetric or trivial irreducible representation (irrep) of the symmetric group S_N ,^{50,59} which will be denoted by A throughout this manuscript.

The global ground state, $|0\rangle$, is also permutationally invariant; therefore, the states $|1_0\rangle$ and

$$\begin{aligned} |1_A\rangle &= \frac{\hat{f}_+^{(0)}}{\sqrt{N}} |0\rangle \\ &= \frac{1}{\sqrt{N}} \sum_{i=1}^N |1_i\rangle, \end{aligned} \quad (5)$$

carry the totally-symmetric irrep as well. On the other hand, the states

$$|1_{B(k)}\rangle = \sum_{n=1}^N c_n^{(k)} |1_n\rangle, \quad (6)$$

where the coefficients $c_n^{(k)}$ fulfill $\sum_{n=1}^N c_n^{(k)} = 0$ and $\sum_{n=1}^N c_n^{(k)*} c_n^{(k')} = \delta_{kk'}$, span the $N - 1$ -dimensional Hilbert subspace corresponding to the standard irrep of S_N , denoted by B , which is orthogonal to the totally-symmetric one.

Since the subspace that the wavefunctions $|1_{B(k)}\rangle$ span is highly degenerate, the choice of basis is not unique.⁶⁰ The most prominent examples of these bases are the Fourier basis:

$$c_n^{(k)} = \frac{1}{\sqrt{N}} \exp\left(2\pi i \frac{(k-1)n}{N}\right), \quad (7)$$

in which $2\pi(k-1)/N$ is a wave vector, and the Schur-Weyl basis, where

$$c_n^{(k)} = \frac{\alpha_n^{(k)}}{\sqrt{k(k-1)}}, \quad (8)$$

with

$$\alpha_n^{(k)} = \begin{cases} -1 & \text{for } 1 \leq n < k \\ k-1 & \text{if } n = k \\ 0 & \text{for } k < n \leq N \end{cases}. \quad (9)$$

TABLE I. SU(2) and SU(3) identifiers of the molecular symmetry-adapted states.

State	J_0	$M_J^{(0)}$	y	SU(3) multiplet
$ 0\rangle$	$N/2$	$-N/2$	$N/3$	$(N, 0)$
$ 1_A\rangle$	$N/2$	$1 - N/2$	$N/3$	$(N, 0)$
$ 1_{B(k)}\rangle$	$N/2 - 1$	$1 - N/2$	$N/3$	$(N - 2, 1)$
$ 1_A^2\rangle$	$N/2$	$2 - N/2$	$N/3$	$(N, 0)$
$ 1_{B(k)}^2\rangle$	$N/2 - 1$	$2 - N/2$	$N/3$	$(N - 2, 1)$
$ 1_{C(k\ell)}^2\rangle$	$N/2 - 2$	$2 - N/2$	$N/3$	$(N - 4, 2)$
$ 2_A\rangle$	$(N - 1)/2$	$(1 - N)/2$	$N/3 - 1$	$(N, 0)$
$ 2_{B(k)}\rangle$	$(N - 1)/2$	$(1 - N)/2$	$N/3 - 1$	$(N - 2, 1)$

The states in the symmetry-adapted basis in eqs. (5) and (6) are also known as Dicke states,^{23,61} $|J_{(0)}, M_J^{(0)}\rangle$, with quantum numbers given by the equations

$$\hat{J}_{(0)}^2 |J_{(0)}, M_J^{(0)}\rangle = J_{(0)}(J_{(0)} + 1) |J_{(0)}, M_J^{(0)}\rangle, \quad (10a)$$

and

$$\hat{J}_0^{(0)} |J_{(0)}, M_J^{(0)}\rangle = M_J^{(0)} |J_{(0)}, M_J^{(0)}\rangle, \quad (10b)$$

where

$$\hat{J}_{(0)}^2 = \left(\hat{J}_0^{(0)}\right)^2 + \frac{1}{2} \left(\hat{J}_+^{(0)} \hat{J}_-^{(0)} + \hat{J}_-^{(0)} \hat{J}_+^{(0)}\right). \quad (11)$$

For reasons that will become evident later, we found our labeling of the irreps more convenient; however, the identification of our notation with the corresponding quantum numbers from angular momentum operators can be found in table I.

In the basis $\{|1_0\rangle, |1_A\rangle, |1_{B(2)}\rangle, |1_{B(3)}\rangle, \dots, |1_{B(N)}\rangle\}$, the Hamiltonian becomes

$$H_1 = \begin{pmatrix} \omega_0 & \sqrt{N}g_{01} & 0 & 0 & \dots & 0 \\ \sqrt{N}g_{10} & \omega_{10} & 0 & 0 & \dots & 0 \\ 0 & 0 & \omega_{10} & 0 & \dots & 0 \\ 0 & 0 & 0 & \omega_{10} & \dots & 0 \\ \vdots & \vdots & \vdots & \vdots & \ddots & \vdots \\ 0 & 0 & 0 & 0 & \dots & \omega_{10} \end{pmatrix} \quad (12)$$

$$= \mathbf{H}_1^{(A)} \oplus \left(\mathbf{1}_{N-1} \otimes \mathbf{H}_1^{(B)}\right),$$

where $\mathbf{H}_1^{(A)}$ is a 2×2 matrix, $\mathbf{H}_1^{(B)} = \omega_{10}$, and $\mathbf{1}_d$ is the d -dimensional identity matrix.

From eq. (12), it becomes clear that the dark states $|1_{B(k)}\rangle$ are eigenfunctions of \hat{H}_1 . The other eigenstates are in the totally-symmetric sub-space:

$$|1_{\pm}\rangle = \pm h_{\pm} |1_0\rangle + h_{\mp} |1_A\rangle, \quad (13)$$

where $+$ and $-$ label the upper and lower polariton, respectively, and $h_{\pm} = \sqrt{\frac{1}{2} \left(1 \pm \frac{\Delta}{\Omega_{10}}\right)}$ are known as Hopfield coeffi-

cients. The corresponding eigenfrequencies are

$$\begin{aligned} \langle 1_{\pm} | \hat{H}_1 | 1_{\pm} \rangle &= \omega_{\pm} \\ &= \frac{\omega_0 + \omega_{10} \pm \Omega_{10}}{2}, \end{aligned} \quad (14)$$

where $\Omega_{10} = \sqrt{\Delta^2 + 4Ng_{01}^2}$ is the Rabi frequency, and $\Delta = \omega_0 - \omega_{10}$ is the detuning. Notice that the use of permutational symmetry arguments to derive the analytical solution of the eigenspectrum of \hat{H}_1 is a drastic simplification of a brute-force numerical diagonalization of a $(N + 1)$ -dimensional matrix, which in the limit of $N = 10^6 - 10^{10}$, as is the case of collective SC, becomes intractable. We shall see how an analogous simplification can be carried out for the second-excitation manifold.

The intensities of spectroscopic signals depend on the off-diagonal matrix elements of the collective dipole operator $\hat{\boldsymbol{\mu}} = \sum_{i=1}^N \hat{\boldsymbol{\mu}}_i$, and the photon mode creation operator \hat{a}_0^{\dagger} . For transitions between the ground state, $|0\rangle$, and the eigenstates in the first excitation manifold we have

$$\langle 1_{\pm} | \hat{\boldsymbol{\mu}} | 0 \rangle = \sqrt{N} h_{\mp} \boldsymbol{\mu}_{10}, \quad (15)$$

$$\langle 1_{B(k)} | \hat{\boldsymbol{\mu}} | 0 \rangle = 0, \quad (16)$$

$$\langle 1_{\pm} | \hat{a}_0^{\dagger} | 0 \rangle = \pm h_{\pm}, \quad (17)$$

and

$$\langle 1_{B(k)} | \hat{a}_0^{\dagger} | 0 \rangle = 0, \quad (18)$$

where $\boldsymbol{\mu}_{10} = \langle 1 | \hat{\boldsymbol{\mu}} | 0 \rangle$ is the dipole moment for the $0 \rightarrow 1$ transition of the bare emitters. Equation (16) can be understood under the consideration that the operator $\hat{\boldsymbol{\mu}}$ is totally-symmetric, and the states $|1_{B(k)}\rangle$ carry an orthogonal irrep.

III. THE SECOND EXCITATION MANIFOLD

The states with two quanta can be of the form

$$|1_i 1_j\rangle = \left(\hat{\boldsymbol{\sigma}}_{j \neq i}^{(0)}\right)^{\dagger} |1_i\rangle, \quad (19)$$

in which the i th and the j th particle are both in their first excited state, or

$$|2_0\rangle = \frac{\hat{a}_0^{\dagger}}{\sqrt{2}} |1_0\rangle, \quad (20a)$$

and

$$|2_{i>0}\rangle = \left(\hat{\boldsymbol{\sigma}}_i^{(1)}\right)^{\dagger} |1_i\rangle, \quad (20b)$$

where the i th particle is in its second excited state. As in the singly excited manifold, all particles not explicitly indicated are in their respective ground state. Notice that a brute-force numerical diagonalization of the second-excitation manifold Hamiltonian \hat{H}_2 would require diagonalization of $\binom{N+2}{2}$ -dimensional matrices, that is unattainable for the large number

N of emitters which concern us in the context of collective SC. Instead, as in the previous section, we will exploit the permutational symmetry arising from the consideration of identical emitters coupled to the cavity.

Just as before, a symmetry-adapted basis can be defined such that there are wavefunctions carrying the totally-symmetric irrep: $|2_0\rangle$,

$$\begin{aligned} |1_0 1_A\rangle &= \hat{a}_0^\dagger |1_A\rangle \\ &= \frac{\hat{J}_+^{(0)}}{\sqrt{N}} |1_0\rangle, \end{aligned} \quad (21)$$

$$\begin{aligned} |1_A^2\rangle &= \frac{\hat{J}_+^{(0)} |1_A\rangle}{\sqrt{2(N-1)}} \\ &= \sqrt{\frac{2}{N(N-1)}} \sum_{i=1}^{N-1} \sum_{j=i+1}^N |1_i 1_j\rangle, \end{aligned} \quad (22)$$

and

$$\begin{aligned} |2_A\rangle &= \hat{J}_+^{(1)} |1_A\rangle \\ &= \frac{1}{\sqrt{N}} \sum_{i=1}^N |2_i\rangle. \end{aligned} \quad (23)$$

There are also wavefunctions carrying the standard irrep:

$$|1_0 1_{B(k)}\rangle = \hat{a}_0^\dagger |1_{B(k)}\rangle, \quad (24)$$

$$\begin{aligned} |1_{B(k)}^2\rangle &= \frac{\hat{J}_+^{(0)} |1_{B(k)}\rangle}{\sqrt{N-2}} \\ &= \sum_{m=1}^{N-1} \sum_{n=m+1}^N c_{mn}^{(k)} |1_m 1_n\rangle, \end{aligned} \quad (25)$$

and

$$\begin{aligned} |2_{B(k)}\rangle &= \hat{J}_+^{(1)} |1_{B(k)}\rangle \\ &= \sum_{n=1}^N c_n^{(k)} |2_n\rangle, \end{aligned} \quad (26)$$

where the coefficients $c_n^{(k)}$ are the same as in eqs. (7) and (8), and the coefficients $c_{mn}^{(k)} = (c_m^{(k)} + c_n^{(k)})/\sqrt{N-2}$ fulfill

$$\sum_{m=1}^{N-1} \sum_{n=m+1}^N c_{mn}^{(k)} = 0, \quad (27a)$$

and

$$\sum_{m=1}^{N-1} \sum_{n=m+1}^N c_{mn}^{(k)} c_{mn}^{(k')*} = \delta_{kk'}. \quad (27b)$$

In the Fourier basis, these coefficients are

$$c_{mn}^{(k)} = \frac{2 \exp[\pi i(k-1) \frac{m+n}{N}]}{\sqrt{N(N-2)}} \cos\left(\pi(k-1) \frac{m-n}{N}\right), \quad (28)$$

while in the Schur-Weyl basis,

$$c_{mn}^{(k)} = \frac{\alpha_{mn}^{(k)}}{\sqrt{(N-2)k(k-1)}}, \quad (29)$$

where

$$\alpha_{mn}^{(k)} = \begin{cases} -2 & \text{for } 1 \leq m < k, \quad 1 < n < k \\ k-2 & \text{for } 1 \leq m < k, \quad n = k \\ -1 & \text{for } 1 \leq m < k, \quad k < n \leq N. \\ k-1 & \text{if } m = k, \quad k < n \leq N \\ 0 & \text{otherwise} \end{cases} \quad (30)$$

Finally, there are wavefunctions,

$$|1_{C(k\ell)}^2\rangle = \sum_{m=1}^{N-1} \sum_{n=m+1}^N c_{mn}^{(k\ell)} |1_m 1_n\rangle, \quad (31)$$

carrying the $N(N-3)/2$ -dimensional irrep that is orthogonal to both the totally-symmetric and the standard irreps. Their coefficients fulfill

$$\sum_{m=1}^{N-1} \sum_{n=m+1}^N c_{mn}^{(k\ell)} = 0, \quad (32a)$$

$$\sum_{m=1}^{N-1} \sum_{n=m+1}^N c_{mn}^{(k\ell)} c_{mn}^{(k'\ell')*} = 0, \quad (32b)$$

and

$$\sum_{m=1}^{N-1} \sum_{n=m+1}^N c_{mn}^{(k\ell)} c_{mn}^{(k'\ell')*} = \delta_{kk'} \delta_{\ell\ell'}. \quad (32c)$$

These coefficients, in the Fourier basis, have the general form

$$c_{mn}^{(k\ell)} = \sum_q \sum_{K(q)} \psi(K_{k\ell}, q_{k\ell}) e^{\pi i K_{k\ell} \frac{m+n}{N}} \cos\left(\pi q_{k\ell} \frac{m-n}{N}\right), \quad (33)$$

where $K_{k\ell}$ labels a center-of-mass wave number, $q_{k\ell}$ identifies a relative wave number, and $\psi(q_{k\ell})$ is a coefficient resulting from symmetrization. The structure of this basis is discussed in greater detail in appendix B. In the Schur-Weyl basis, the coefficients are given by

$$c_{mn}^{(k\ell)} = -\frac{\alpha_{mn}^{(k\ell)}}{\sqrt{k(k-1)(\ell-2)(\ell-3)}}, \quad (34)$$

with

$$\alpha_{mn}^{(k\ell)} = \begin{cases} -2 & \text{for } 1 \leq m < k, \quad 1 < n < k \\ k-2 & \text{for } 1 \leq m < k, \quad n = k \\ -1 & \text{for } 1 \leq m < k, \quad k < n < \ell \\ \ell-3 & \text{for } 1 \leq m < k, \quad n = \ell \\ k-1 & \text{for } m = k, \quad k < n < \ell \\ -(k-1)(\ell-3) & \text{if } m = k, \quad n = \ell \\ 0 & \text{otherwise} \end{cases} \quad (35)$$

We note that the involvement of $\hat{J}_+^{(1)}$ in eqs. (23) and (26) implies that the SU(2) algebra with operators $\hat{J}_x^{(0)}$ is insufficient to characterize the states with two excitations in the same emitter.⁶² These states need labels from the SU(3) algebra for their correct identification. In table I, we present these labels, including the eigenvalues, y , of the operator

$$\hat{Y} = \frac{2}{3} \left([\hat{J}_+^{(1)}, \hat{J}_-^{(1)}] - \hat{J}_0^{(0)} \right), \quad (36)$$

usually known as hypercharge in the literature of particle physics.⁶³ We also require labels for the SU(3) irrep or multiplet; the methods to identify them can be found elsewhere.⁶⁴ As we can see, J_0 is useful to identify the symmetry of states with at most one excitation per emitter, but is not capable of classifying the remaining states. On the other hand, the irreps of SU(3) thoroughly fulfill this job. However, keeping track of that many quantum numbers is cumbersome for the purposes of this work, and the A, B, C scheme here introduced conveys the important information in a more condensed way.

Up to this point, we know that the matrix element

$$\langle \Psi_\Gamma | \hat{H}_2 | \Psi_{\Gamma'} \rangle = 0, \quad (37)$$

if $\Gamma \neq \Gamma'$, where \hat{H}_2 is the Hamiltonian with $n_{\text{exc}} = 2$, and $|\Psi_\Gamma\rangle$ is a symmetrized state carrying the irrep Γ which can be either A, B or C.

The form of the Hamiltonian in the subspaces carrying the irreps A and B depends on the considered spectrum of the emitters, and will be discussed in the following sections. On the other hand, the states $|1_{C(k\ell)}^2\rangle$ do not couple to the EM mode in any capacity nor among themselves, and are therefore eigenstates of \hat{H}_2 in every model discussed below, i.e.,

$$\langle 1_{C(k\ell)}^2 | \hat{H}_2 | 1_{C(k'\ell')}^2 \rangle = 2\omega_{10} \delta_{kk'} \delta_{\ell\ell'}; \quad (38)$$

as such, they will not be discussed in the next subsections.

Figure 1 illustrates the distribution of every spectral configuration among the irreps. To be specific, the Hamiltonian matrix in the second excitation manifold decomposes according to

$$\mathbf{H}_2 = \mathbf{H}_2^{(A)} \oplus \left(\mathbf{1}_{N-1} \otimes \mathbf{H}_2^{(B)} \right) \oplus \left(\mathbf{1}_{N(N-3)/2} \otimes \mathbf{H}_2^{(C)} \right), \quad (39)$$

where the dimensions of $\mathbf{H}_2^{(A)}$ and $\mathbf{H}_2^{(B)}$ depend upon the particular energetic structure of the emitters, and $\mathbf{H}_2^{(C)} = 2\omega_{10}$.

A. Tavis-Cummings

If the emitters are well-approximated by two-level systems, the matrix elements of the Hamiltonian for the doubly excited manifold are

$$\langle 2_0 | \hat{H}_2 | 2_0 \rangle = 2\omega_0, \quad (40a)$$

$$\langle 2_0 | \hat{H}_2 | 1_i 1_j \rangle = \sqrt{2} g_{01} \delta_{i0}, \quad (40b)$$

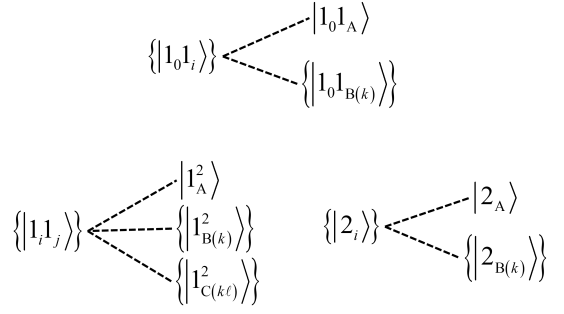


FIG. 1. Distribution of states in the doubly excited manifold among irreps.

$$\langle 1_i 1_j | \hat{H}_2 | 2_0 \rangle = \sqrt{2} g_{10} \delta_{i0}, \quad (40c)$$

and

$$\langle 1_i 1_j | \hat{H}_2 | 1_{i'} 1_{j'} \rangle = \begin{cases} \omega_0 + \omega_{10} & \text{if } i = i' = 0, \quad j = j' \\ 2\omega_{10} & \text{if } i = i' \neq 0, \quad j = j' \neq 0 \\ g_{01} & \text{if } i = 0 \neq i', \quad j = j' \\ g_{10} & \text{if } i \neq 0 = i', \quad j = j' \\ 0 & \text{otherwise} \end{cases}. \quad (40d)$$

In turn, the matrix in the totally-symmetric subspace, i.e., with the symmetrized basis $\{|2_0\rangle, |1_0 1_A\rangle, |1_A^2\rangle\}$, is

$$\mathbf{H}_{2,TC}^{(A)} = \begin{pmatrix} 2\omega_0 & \sqrt{2N}g_{10} & 0 \\ \sqrt{2N}g_{01} & \omega_0 + \omega_{10} & \sqrt{2(N-1)}g_{10} \\ 0 & \sqrt{2(N-1)}g_{01} & 2\omega_{10} \end{pmatrix} \quad (41)$$

For states carrying the standard irrep, $\{|1_0 1_{B(k)}\rangle, |1_{B(k)}^2\rangle\}$, the corresponding Hamiltonian matrix is

$$\mathbf{H}_{2,TC}^{(B)} = \begin{pmatrix} \omega_0 + \omega_{10} & \sqrt{N-2}g_{10} \\ \sqrt{N-2}g_{01} & 2\omega_{10} \end{pmatrix} \quad (42)$$

Notice that, as opposed to the singly excited manifold, the sub-space carrying the standard irrep of the doubly excited Hamiltonian is no longer diagonal in the symmetry-adapted basis.

Diagonalization of $\mathbf{H}_{2,TC}^{(A)}$ gives rise to the so-called bipolaritonic states^{38,42,49,65}

$$\hat{H}_2 |2_\pm\rangle = \omega_{2\pm} |2_\pm\rangle, \quad (43a)$$

and

$$\hat{H}_2 |1_+ 1_-\rangle = \omega_{1_+ 1_-} |1_+ 1_-\rangle. \quad (43b)$$

Eigenstates and eigenfrequencies of this 3×3 matrix can be easily obtained numerically. Analytical expressions, however, are cumbersome (see appendix A) unless the reasonable approximation $N \gg 1$ is considered, in which case:

$$|2_\pm\rangle_{TC} = h_\pm^2 |2_0\rangle \pm \sqrt{2} h_+ h_- |1_0 1_A\rangle + h_\mp^2 |1_A^2\rangle, \quad (44)$$

and

$$\begin{aligned} |1_+1_-\rangle_{\text{TC}} &= \sqrt{2}h_+h_-(-|2_0\rangle + |1_A^2\rangle) \\ &+ (h_+^2 - h_-^2)|1_01_A\rangle. \end{aligned} \quad (45)$$

The eigenvectors of $\mathbf{H}_{2,\text{TC}}^{(\text{B})}$ give the coefficients for the oftentimes referred to as ‘‘upper(lower) polariton-dark states’’:^{38,42}

$$|1_{\pm}1_{\text{B}(k)}\rangle_{\text{TC}} = \pm h_{\pm}|1_01_{\text{B}(k)}\rangle + h_{\mp}|1_{\text{B}(k)}^2\rangle, \quad (46)$$

which fulfill

$$\hat{H}_2|1_{\pm}1_{\text{B}(k)}\rangle_{\text{TC}} = \omega_{1_{\pm}1_{\text{B}}} |1_{\pm}1_{\text{B}(k)}\rangle_{\text{TC}}. \quad (47)$$

The eigenfrequencies are tabulated in table II, while the matrix elements of transition operators between the eigenstates in the first excitation manifold and those in eqs. (44) to (46) are included in tables III to VI. The analytical expressions for the solutions with arbitrary N can be found in Appendix A.

B. Harmonic limit

When two levels are not enough to depict the structure of the emitters, the simplest way to add complexity to the system is by considering the emitters as harmonic oscillators, i.e., with evenly-spaced levels in their energy spectrum. This assumption is valid for modes related to bonds with high dissociation energies. In this scenario, the new light-matter Hamiltonian incorporates additional matrix elements given by

$$\langle 2_{i>0} | \hat{H}_2 | 2_j \rangle = 2\omega_{10}\delta_{ij}, \quad (48a)$$

$$\langle 1_01_i | \hat{H}_2 | 2_j \rangle = \sqrt{2}g_{01}\delta_{ij}, \quad (48b)$$

and

$$\langle 2_i | \hat{H}_2 | 1_01_j \rangle = \sqrt{2}g_{10}\delta_{ij}. \quad (48c)$$

Notice that the harmonic approximation assumes $\omega_{12} = \omega_{10}$ and $g_{12} = \sqrt{2}g_{01}$.

With the new symmetrized contributions to the space of functions, namely $|2_A\rangle$ for $\mathbf{H}_2^{(\text{A})}$, and $\{|2_{\text{B}(k)}\rangle\}$ for $\mathbf{H}_2^{(\text{B})}$, the expanded Hamiltonian matrices are

$$\mathbf{H}_{2,\text{HO}}^{(\text{A})} = \begin{pmatrix} 2\omega_0 & \sqrt{2N}g_{10} & 0 & 0 \\ \sqrt{2N}g_{01} & \omega_0 + \omega_{10} & \sqrt{2(N-1)}g_{10} & \sqrt{2}g_{10} \\ 0 & \sqrt{2(N-1)}g_{01} & 2\omega_{10} & 0 \\ 0 & \sqrt{2}g_{01} & 0 & 2\omega_{10} \end{pmatrix}, \quad (49)$$

for the totally-symmetric irrep, and

$$\mathbf{H}_{2,\text{HO}}^{(\text{B})} = \begin{pmatrix} \omega_0 + \omega_{10} & \sqrt{N-2}g_{10} & g_{21} \\ \sqrt{N-2}g_{01} & 2\omega_{10} & 0 \\ g_{12} & 0 & 2\omega_{10} \end{pmatrix}, \quad (50)$$

for the standard irrep.

While the separation of the Hamiltonian accomplished with this approach significantly facilitates the numerical diagonalization, a simpler approach to obtain analytical results can be achieved by noticing that a harmonic bi-linear Hamiltonian can always be written as a sum of normal harmonic modes. In other words, the Hamiltonian of the system becomes

$$\begin{aligned} \hat{H}_{\text{HO}} &= \omega_0 \hat{a}_0^\dagger \hat{a}_0 + \omega_{10} \sum_{i=1}^N \hat{a}_i^\dagger \hat{a}_i \\ &+ \sum_{i=1}^N \left(g_{10} \hat{a}_i^\dagger \hat{a}_0 + g_{01} \hat{a}_0^\dagger \hat{a}_i \right), \end{aligned} \quad (51)$$

where $\hat{a}_i = \sum_{v=0}^{\infty} \sqrt{v+1} \hat{\sigma}_i^{(v)}$ is the bosonic annihilation operator acting on the i th emitter. A set of symmetrized operators can be defined such that the Hamiltonian becomes

$$\begin{aligned} \hat{H}_{\text{HO}} &= \omega_0 \hat{a}_0^\dagger \hat{a}_0 + \omega_{10} \hat{a}_A^\dagger \hat{a}_A + \sqrt{N} \left(g_{10} \hat{a}_A^\dagger \hat{a}_0 + g_{01} \hat{a}_0^\dagger \hat{a}_A \right) \\ &+ \omega_{10} \sum_{k=2}^N \hat{a}_{\text{B}(k)}^\dagger \hat{a}_{\text{B}(k)}, \end{aligned} \quad (52)$$

with creation operators $\hat{a}_A^\dagger = \sum_{v=0}^{\infty} \sqrt{v+1} \hat{J}_+^{(v)} / \sqrt{N}$, and $\hat{a}_{\text{B}(k)}^\dagger = \sum_{n=1}^N c_n^{(k)} \hat{a}_n^\dagger$, where the coefficients $c_n^{(k)}$ are the same as in eq. (6). Furthermore, defining the polaritonic modes through the creation operators $\hat{a}_{\pm}^\dagger = \pm h_{\pm} \hat{a}_0^\dagger + h_{\mp} \hat{a}_A^\dagger$, allows to rewrite the Hamiltonian as

$$\hat{H}_{\text{HO}} = \omega_+ \hat{a}_+^\dagger \hat{a}_+ + \omega_- \hat{a}_-^\dagger \hat{a}_- + \omega_{10} \sum_{k=2}^N \hat{a}_{\text{B}(k)}^\dagger \hat{a}_{\text{B}(k)}. \quad (53)$$

Since the modes defined by this Hamiltonian are independent, any combination of creation operators applied to the ground-state will generate an eigenstate. Consequently, for the totally-symmetric subspace,

$$\begin{aligned} |2_{\pm}\rangle_{\text{HO}} &= \frac{(\hat{a}_{\pm}^\dagger)^2}{\sqrt{2}} |0\rangle \\ &= h_{\pm}^2 |2_0\rangle \pm \sqrt{2}h_+h_- |1_01_A\rangle \\ &+ h_{\mp}^2 \left(\frac{\sqrt{N-1}|1_A^2\rangle + |2_A\rangle}{\sqrt{N}} \right), \end{aligned} \quad (54a)$$

$$\begin{aligned} |1_+1_-\rangle_{\text{HO}} &= \hat{a}_+^\dagger \hat{a}_-^\dagger |0\rangle \\ &= -\sqrt{2}h_+h_- |2_0\rangle + (h_+^2 - h_-^2) |1_01_A\rangle \\ &+ \sqrt{2}h_+h_- \left(\frac{\sqrt{N-1}|1_A^2\rangle + |2_A\rangle}{\sqrt{N}} \right) \end{aligned} \quad (54b)$$

and

$$\begin{aligned} |2_{DA}\rangle_{\text{HO}} &= \frac{1}{\sqrt{N-1}} \sum_{k=2}^N \frac{(\hat{a}_{\text{B}(k)}^\dagger)^2}{\sqrt{2}} |0\rangle \\ &= \frac{-|1_A^2\rangle + \sqrt{N-1}|2_A\rangle}{\sqrt{N}}. \end{aligned} \quad (54c)$$

The eigenstates carrying the standard representation are

$$\begin{aligned} |1_{\pm}1_{B(k)}\rangle_{\text{HO}} &= \hat{a}_{\pm}^{\dagger}\hat{a}_{B(k)}|0\rangle = \hat{a}_{B(k)}^{\dagger}\hat{a}_{\pm}|0\rangle \\ &= \pm h_{\pm}|1_01_{B(k)}\rangle \\ &\quad + h_{\mp}\left(\frac{\sqrt{N-2}|1_{B(k)}^2\rangle + \sqrt{2}|2_{B(k)}\rangle}{\sqrt{N}}\right) \end{aligned} \quad (55a)$$

and

$$|2_{DB(k)}\rangle_{\text{HO}} = \frac{-\sqrt{2}|1_{B(k)}^2\rangle + \sqrt{N-2}|2_{B(k)}\rangle}{\sqrt{N}}. \quad (55b)$$

The states $|2_{DA}\rangle$ and $|2_{DB(k)}\rangle$ are purely molecular and account for the addition of states of the form $|2_i\rangle$ to the Hilbert space.

The emerging eigenvalues are on display in table II, and the transition intensities between first and second excitation manifolds for this model are summarized in tables III to VI. Figure 2 compares the behavior of the energy spectrum for the TC model and the harmonic approximation as functions of the number of coupled emitters and detuning. As it can be seen, the TC model and the harmonic approximation yield indistinguishable results as the number of emitters increases. To explain this observation, we remark that the interaction between the cavity and the $1 \rightarrow 2$ transition in the emitters is not extensive, as opposed to the $0 \rightarrow 1$ transition. Therefore, although the overall light-matter coupling in the multi-level system is stronger than in the TC model, the contribution from the additional level gets diluted as the ensemble grows. We emphasize again the emergence of states in the multi-level case, $|2_{DA}\rangle$ and $|2_{DB}\rangle$, whose lack of photonic character makes them impervious to detuning.

C. General (anharmonic) case.

More realistically, emitters deviate from the behavior of harmonic oscillators. In particular, for molecular vibrations, there is a mechanical anharmonicity reflecting that vibrational energy levels are not evenly spaced, i.e.,

$$\omega_{12} = \omega_{10}(1 - \chi), \quad (56)$$

where χ is the mechanical anharmonicity constant. Additionally, an electrical anharmonicity constant, γ , can also be defined stemming from

$$g_{12} = \sqrt{2}g_{01}(1 + \gamma). \quad (57)$$

These anharmonicities are generally present in electronic transitions as well. Notice also that the TC model effectively corresponds to the anharmonic case with $\chi = 0$ and $\gamma = -1$.

In terms of these parameters, the matrix elements of the light-matter Hamiltonian need to be updated to

$$\langle 2_{i>0} | \hat{H}_2 | 2_j \rangle = (\omega_{10} + \omega_{21})\delta_{ij}, \quad (58a)$$

$$\langle 1_0 1_j | \hat{H}_2 | 2_j \rangle = g_{12}\delta_{ij}, \quad (58b)$$

$$\langle 2_i | \hat{H}_2 | 1_0 1_j \rangle = g_{21}\delta_{ij}. \quad (58c)$$

In the symmetry-adapted basis they become

$$\langle 2_A | \hat{H}_2 | 2_A \rangle = \omega_{10} + \omega_{21}, \quad (59a)$$

$$\langle 2_A | \hat{H}_2 | 1_0 1_A \rangle = g_{12}, \quad (59b)$$

and

$$\langle 1_0 1_A | \hat{H}_2 | 2_A \rangle = g_{21}, \quad (59c)$$

for the totally-symmetric irrep, and

$$\langle 2_{B(k)} | \hat{H}_2 | 2_{B(k')} \rangle = (\omega_{10} + \omega_{21})\delta_{kk'}, \quad (60a)$$

$$\langle 2_{B(k)} | \hat{H}_2 | 1_0 1_{B(k')} \rangle = g_{12}\delta_{kk'}, \quad (60b)$$

and

$$\langle 1_0 1_{B(k)} | \hat{H}_2 | 2_{B(k')} \rangle = g_{21}\delta_{kk'}, \quad (60c)$$

for the standard irrep. The effects of anharmonicities can thus be introduced as corrections to the harmonic Hamiltonian matrices in eqs. (49) and (50). Explicitly, the full Hamiltonian matrices, carrying the irrep Γ , in the second-excitation manifold read

$$\mathbf{H}_2^{(\Gamma)} = \mathbf{H}_{2,\text{HO}}^{(\Gamma)} + \mathbf{H}_2^{\prime(\Gamma)}, \quad (61)$$

where

$$\mathbf{H}_2^{\prime(A)} = \begin{pmatrix} 0 & 0 & 0 & 0 \\ 0 & 0 & 0 & \gamma\sqrt{2}g_{10} \\ 0 & 0 & 0 & 0 \\ 0 & \gamma\sqrt{2}g_{01} & 0 & -\chi\omega_{10} \end{pmatrix} \quad (62)$$

and

$$\mathbf{H}_2^{\prime(B)} = \begin{pmatrix} 0 & 0 & \gamma\sqrt{2}g_{10} \\ 0 & 0 & 0 \\ \gamma\sqrt{2}g_{01} & 0 & -\chi\omega_{10} \end{pmatrix}, \quad (63)$$

are the anharmonic corrections with $\Gamma = A$ and B , respectively. The interaction between levels according to their symmetry is summarized in fig. 3.

To analyze the effect of anharmonicity in the energy spectra we consider, without loss of generality, the emitters as Morse oscillators, i.e., the mass-normalized normal-mode elongation, x , is subject to a potential energy of the form⁶⁶

$$V(x) = \hbar\omega_{10}\frac{(1+\chi)^2}{2\chi}\left[1 - \exp\left(-\sqrt{\frac{\omega_{10}\chi}{\hbar}}x\right)\right]^2. \quad (64)$$

For this system, the electrical and mechanical anharmonicities are related through⁶⁷

$$\gamma = \frac{1}{2}\sqrt{\frac{(1+\chi)(16-\chi^2)}{2(2+\chi)}} - 1. \quad (65)$$

Figure 4 compares the exact energy spectra of totally-symmetric states as a function of anharmonicity for several

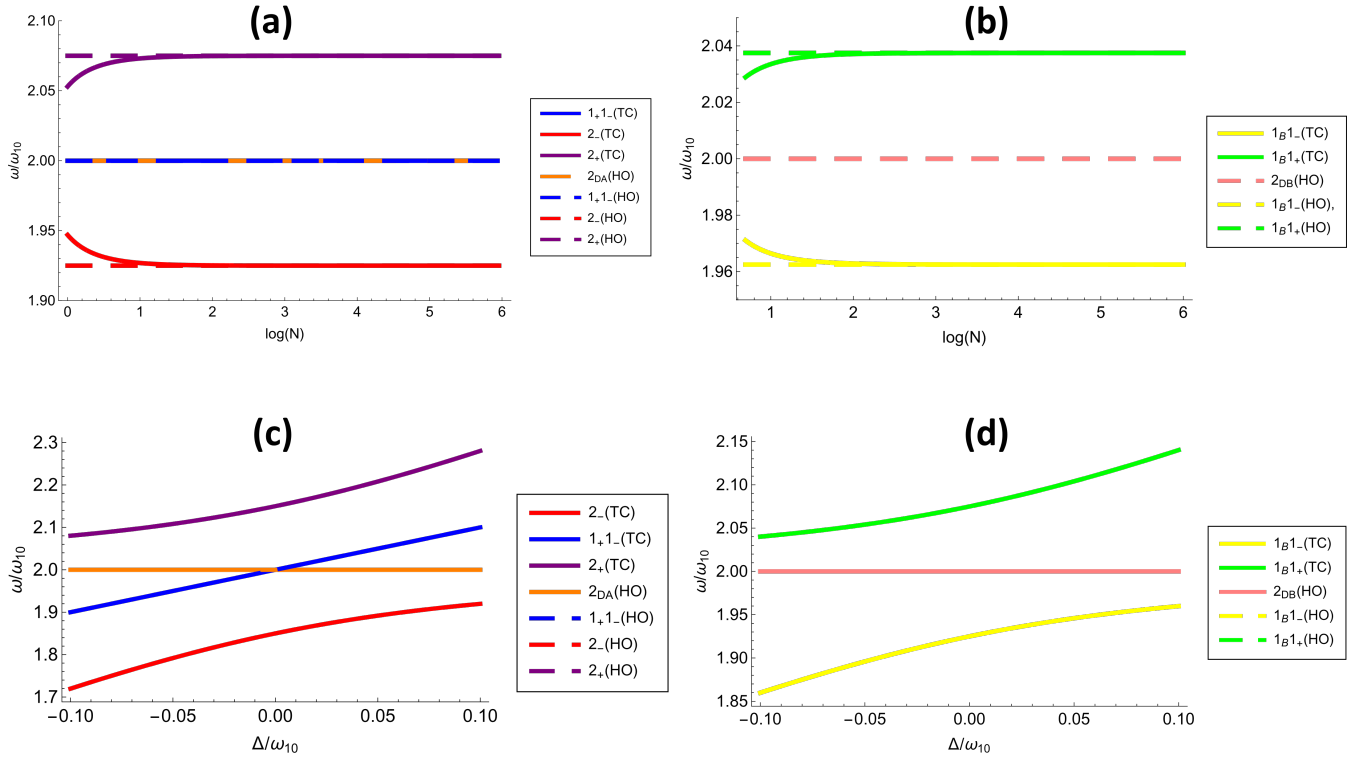


FIG. 2. Energy spectrum of the doubly excited manifold in the Tavis-Cummings (TC) and the harmonic oscillator (HO) models. Spectra of totally-symmetric states (a) and states carrying the standard irrep (b) as a function of the number of emitters, N , for a cavity in resonance with the $0 \rightarrow 1$ vibrational transition. Spectra of totally-symmetric states (c) and states carrying the standard irrep (d) as a function of the detuning between the cavity and the $0 \rightarrow 1$ transition, for $N = 10^9$. All plots were calculated with constant collective coupling amplitude of $7\omega_{10}/100$. Notice that (b) starts at $\log(N) > 0$ because there are no states carrying the standard representation for $N = 1$. Also, notice that the 2_{DA} and 2_{DB} states are only defined for the HO model, as the TC model does not afford states with two excitations in the same emitter. Finally, the lack of photonic character for 2_{DA} and 2_{DB} implies that they remain dispersionless as a function of detuning Δ .

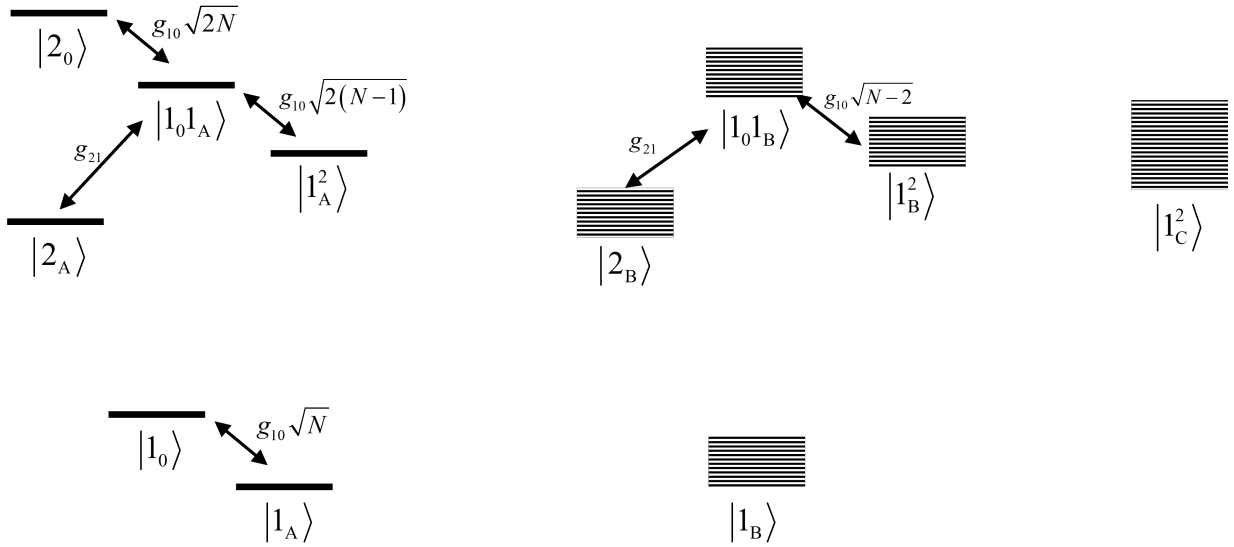


FIG. 3. Interaction scheme among levels in the singly and doubly excited manifolds. States carrying the totally-symmetric (A) irreducible representation are non-degenerate, while states with the standard (B) and C irreps are $(N-1)$ -fold and $N(N-3)/2$ -fold degenerate, respectively. States with labels 2_A and 2_B do not appear in the Tavis-Cummings model.

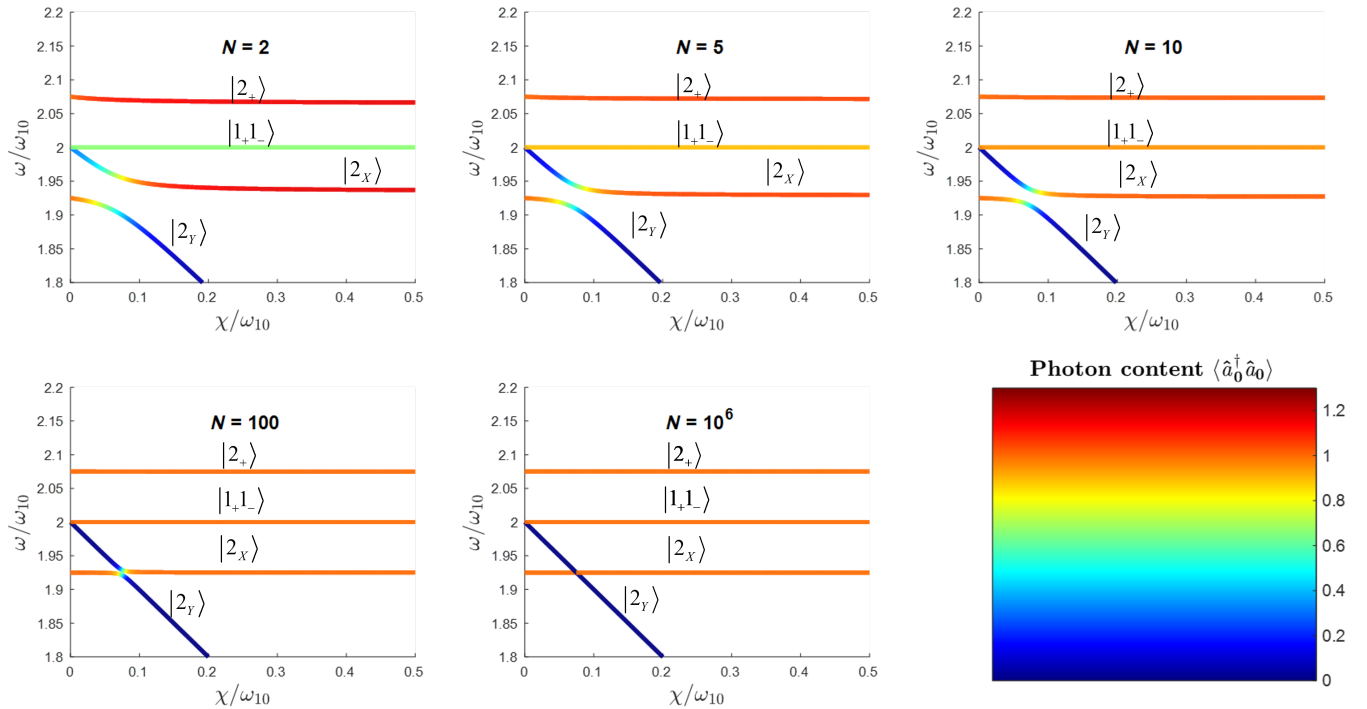


FIG. 4. Exact energy spectrum of doubly-excited totally-symmetric eigenstates as a function of anharmonicity, χ , for several numbers of Morse emitters. Resonant case ($\omega_0 = \omega_{10}$). The labeling identifies the frequencies of the adiabatic eigenstates as a function of χ/ω_{10} . Since the states $|2_+\rangle$ and $|1_+1_-\rangle$ are well-separated in energy, they have been labeled to reflect that they are very similar to the corresponding harmonic eigenstates. The $|2_x\rangle$ and $|2_y\rangle$ adiabatic eigenstates show avoided crossings resulting from anharmonic mixing of the harmonic states $|2_{DA}\rangle$ and $|2_-\rangle$. In all cases, $|2_x\rangle \approx |2_{DA}\rangle$ and $|2_y\rangle \approx |2_-\rangle$ for $\chi \rightarrow 0$, and $|2_x\rangle \approx |2_-\rangle$ and $|2_y\rangle \approx |2_{DA}\rangle$ for large χ . The photon content is evaluated as the expectation value of the number operator $\hat{a}_0^\dagger \hat{a}_0$. Notice that, for large N , the avoided crossings giving rise to the $|2_x\rangle$ and $|2_y\rangle$ states are essentially crossings between the very anharmonic state $|2_{DA}\rangle$ and the bipolariton $|2_-\rangle$. These crossings are loci of two-photon absorption enhancement.

values of N obtained through numerical diagonalization of $\mathbf{H}_2^{(A)}$.

As can be seen, the harmonic states $|2_-\rangle$ and $|2_{DA}\rangle$ interact anharmonically with a coupling strength determined by the single-molecule light-matter coupling constant g_{21} . Therefore, it is possible to find a set of parameters in the Hamiltonian for which these states are near-resonant for large N , which is the limit that concerns us for collective SC. Under this condition, the absorption of two photons with the frequency of the $|0\rangle \rightarrow |1_-\rangle$ transition will experience an enhancement, as discussed in refs. 40 and 49. This phenomenon can be understood as follows: the bipolariton $|2_-\rangle$ provides an optical window to funnel energy efficiently into the anharmonic $|2_{DA}\rangle$ state.^{48,49} The effect can be observed when $\omega_{2-} \approx 2\omega_{10} - \chi$. At light-matter resonance with the fundamental transition ($\omega_0 = \omega_{10}$), this condition translates into the more intuitive $\Omega_{10} \approx \chi$, i.e., the Rabi splitting must be tuned to match the anharmonic shift. Note that the bipolariton $|2_-\rangle$ is the only possible optical window to resonate with $|2_{DA}\rangle$ when $\omega_0 = \omega_{10}$. However, if the photon is negatively detuned from the fundamental transition, $\omega_0 < \omega_{10}$, a second bipolariton $|1_+1_-\rangle$ can also be in resonance with $|2_{DA}\rangle$, as shown in fig. 5. This effect was not discussed in Ref. 49, and should

provide an extra tuning parameter to enhance multiphoton absorption processes in polaritonic systems. The conditions for enhanced two-photon absorption (TPA) are better illustrated in the correlation diagrams of fig. 6.

The calculations above show that, as opposed to the case of linear response, simulations with small N are not a reliable representation of the nonlinear optics of systems under collective SC for anharmonicities up to one order of magnitude larger than the Rabi splitting, even if the intensity of the total coupling, $\sqrt{N}g_{10}$, is fixed to match experimental values of Ω_{10} . Thus, we believe that the interpretation of experimental spectra as reported in refs. 28 and 43 using a single-molecule model is worth revisiting.

While the numerical results above shed much light on the physics of the problem for all ranges of anharmonicity, it is illuminating to carry out a perturbation theory analysis for small values of χ to obtain closed approximate expressions for eigenvalues and eigenvectors of \hat{H}_2 . To zeroth order, we have $|\Psi\rangle^{(0)} = |\Psi\rangle_{\text{HO}}$. The first-order corrections to the eigenfrequencies of the HO limit are included in table II. The $O(\chi, \gamma)$ corrections to the doubly excited polaritonic modes are computed to be

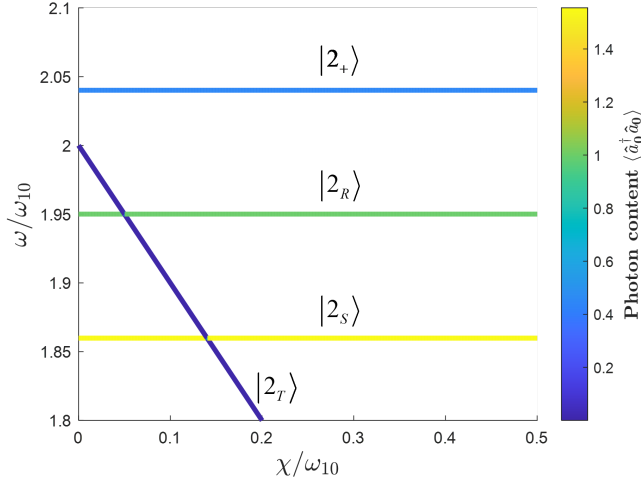


FIG. 5. Analogous plot to fig. 4, panel $N = 10^6$, except that the cavity is negatively detuned ($\omega_0 = 0.95\omega_{10}$). The eigenstate $|2_+\rangle$ is well-separated in energy and has been labeled to reflect that it is very similar to the corresponding harmonic eigenstate. The $|2_R\rangle$, $|2_S\rangle$, $|2_T\rangle$ adiabatic eigenstates show weakly (because of large N) avoided crossings resulting from anharmonic mixing of harmonic states $|2_{DA}\rangle$, $|1_+1_-\rangle$, and $|2_-\rangle$. Three anharmonicity regimes can be recognized: small χ ($|2_R\rangle \approx |2_{DA}\rangle$, $|2_S\rangle \approx |1_+1_-\rangle$, and $|2_T\rangle \approx |2_-\rangle$), intermediate χ ($|2_R\rangle \approx |1_+1_-\rangle$, $|2_S\rangle \approx |2_{DA}\rangle$, and $|2_T\rangle \approx |2_-\rangle$), and large χ ($|2_R\rangle \approx |1_+1_-\rangle$, $|2_S\rangle \approx |2_-\rangle$, and $|2_T\rangle \approx |2_{DA}\rangle$). The avoided crossings occur at resonances between the very anharmonic $|2_{DA}\rangle$ with the bipolaritons $|1_+1_-\rangle$ and $|2_-\rangle$, the latter of which features a significant photonic content. These crossings are the loci of two-photon absorption enhancement. Notice that, owing to the negative detuning, there are two (rather than just one) such crossings, as opposed to the resonant case shown in fig. 4.

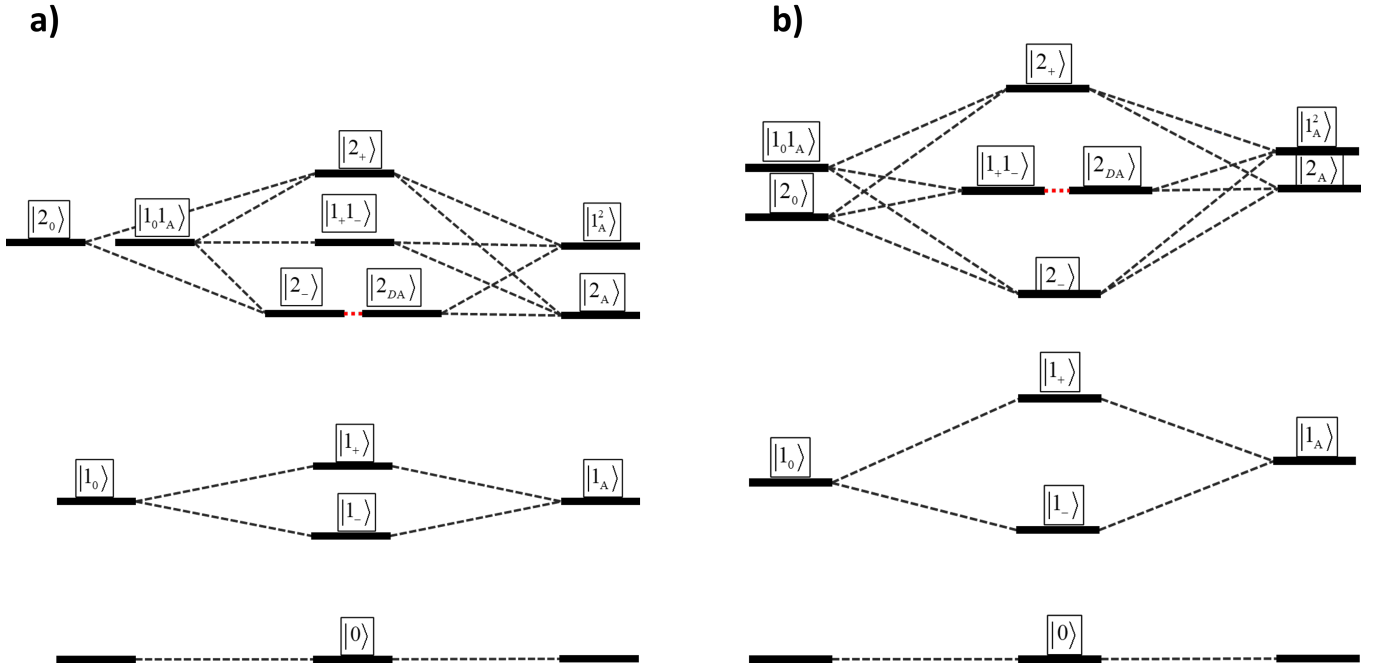


FIG. 6. Correlation diagrams of polaritonic states under the conditions that afford enhanced TPA. (a) If the photon mode is resonant with the $0 \rightarrow 1$ molecular transition (i.e. $\omega_0 = \omega_{10}$), enhancement of TPA occurs when $\omega_{2-} = \omega_{10} + \omega_{21}$ due to anharmonic coupling between the bipolariton $|2_-\rangle$ and the anharmonic state $|2_{DA}\rangle$ (red dotted line). (b) If the photon mode is negatively detuned from the $0 \rightarrow 1$ molecular transition (i.e. $\omega_0 < \omega_{10}$), enhancement of TPA can also occur when $\omega_{1_+1_-} = \omega_{10} + \omega_{21}$ due to anharmonic coupling between the bipolariton $|1_+1_-\rangle$ and the anharmonic state $|2_{DA}\rangle$ (red dotted line).

$$\begin{pmatrix} \langle 2_0 | \\ \langle 1_0 1_A | \\ \langle 1_A^2 | \\ \langle 2_A | \end{pmatrix} |2_{\pm}\rangle^{(1)} = \frac{h_{\mp}^2}{2N\Omega_{10}} \begin{pmatrix} h_+^2 h_-^2 [\pm 3\chi\omega_{10} + 2(h_{\mp}^2 - 5h_{\pm}^2)\gamma\Omega_{10}] \\ \sqrt{2}h_+h_- [(2h_{\mp}^2 - h_{\pm}^2)\chi\omega_{10} \pm 2(h_{\mp}^2 + 2h_{\pm}^2 - 6h_+^2h_-^2)\gamma\Omega_{10}] \\ h_{\mp}^2 \sqrt{\frac{N-1}{N}} \left[\frac{(h_-^2 - h_+^2 \pm 3h_+^2h_-^2)}{h_{\pm}^2} \right] \chi\omega_{10} + 2(2h_{\pm}^2 - h_{\mp}^2 - 6h_+^2h_-^2)\gamma\Omega_{10} \\ \frac{1}{\sqrt{N}} \left\{ \mp \frac{N+h_{\mp}^2(h_{\pm}^2 - h_{\mp}^2 - 3h_+^2h_-^2)}{h_{\pm}^2} \chi\omega_{10} + 2[N + 2h_{\mp}^2(2h_{\pm}^2 - h_{\mp}^2 - 6h_+^2h_-^2)]\gamma\Omega_{10} \right\} \end{pmatrix}. \quad (66)$$

For non-zero detuning, the corrections to the remaining totally-symmetric eigenstates are

$$\begin{pmatrix} \langle 2_0 | \\ \langle 1_0 1_A | \\ \langle 1_A^2 | \\ \langle 2_A | \end{pmatrix} |1_+ 1_-\rangle^{(1)} = \frac{2h_+ h_-}{N\Omega_{10}} \begin{pmatrix} -\sqrt{2}h_+^2 h_-^2 \gamma\Omega_{10} \\ h_+ h_- [\chi\omega_{10} - (h_+^2 - h_-^2) \gamma\Omega_{10}] \\ \sqrt{\frac{2(N-1)}{N}} h_+^2 h_-^2 \left(\frac{2}{h_+^2 - h_-^2} \chi\omega_{10} - 3\gamma\Omega_{10} \right) \\ -\frac{1}{\sqrt{2N}} \left[\frac{N-4h_+^2 h_-^2}{h_+^2 - h_-^2} \chi\omega_{10} + (N-6h_+^2 h_-^2) \gamma\Omega_{10} \right] \end{pmatrix} \quad (67)$$

and

$$\begin{pmatrix} \langle 2_0 | \\ \langle 1_0 1_A | \\ \langle 1_A^2 | \\ \langle 2_A | \end{pmatrix} |2_{DA}\rangle^{(1)} = \frac{\sqrt{N-1}}{2N\Omega_{10}} \begin{pmatrix} \frac{1}{h_-^2 - h_+^2} \chi\omega_{10} \\ \frac{\sqrt{2}}{h_+ h_-} \chi\omega_{10} \\ \sqrt{\frac{N-1}{N}} \left(\frac{1-5h_-^2 h_+^2}{h_+^2 h_-^2 (h_-^2 - h_+^2)} \chi\omega_{10} - 2\gamma\Omega_{10} \right) \\ \frac{1}{\sqrt{N}} \left(\frac{1-5h_-^2 h_+^2}{h_+^2 h_-^2 (h_-^2 - h_+^2)} \chi\omega_{10} - 2\gamma\Omega_{10} \right) \end{pmatrix}. \quad (68)$$

Under resonant conditions, these two states are degenerate in the harmonic limit. After lifting the degeneracy, to zeroth order, these states become

$$|1_+ 1_-\rangle^{(0)} = \frac{\sqrt{N-1}|2_0\rangle - \sqrt{N}|1_A^2\rangle}{\sqrt{2N-1}} \quad (69)$$

$$|2_{DA}\rangle^{(0)} = -\frac{\sqrt{N}|2_0\rangle + \sqrt{N-1}|1_A^2\rangle}{\sqrt{2N(2N-1)}} + \sqrt{\frac{2N-1}{2N}} |2_A\rangle. \quad (70)$$

After this procedure, there are no first-order corrections for the state $|1_+ 1_-\rangle$; on the other hand,

$$|2_{DA}\rangle^{(1)} = \frac{\sqrt{2N-1}}{2N\Omega_{10}} \left(-\frac{\gamma\Omega_{10}}{\sqrt{2}} |2_0\rangle + \chi\omega_{10} |1_0 1_A\rangle - \gamma\Omega_{10} \frac{\sqrt{N-1}|1_A^2\rangle + |2_A\rangle}{\sqrt{2N}} \right). \quad (71)$$

For states carrying the standard irrep, the corrections of first-order in anharmonicity are

$$\begin{pmatrix} \langle 1_0 1_{B(k)} | \\ \langle 1_{B(k)}^2 | \\ \langle 2_{B(k)} | \end{pmatrix} |1_{\pm} 1_{B(k)}\rangle^{(1)} = \frac{\sqrt{2}h_{\mp}}{N\Omega_{10}} \begin{pmatrix} \sqrt{2}h_+ h_- [\chi\omega_{10} - (h_+^2 - h_-^2) \gamma\Omega_{10}] \\ h_{\mp}^2 \sqrt{\frac{2(N-2)}{N}} \left[\pm \left(\frac{2h_{\pm}^2 + h_{\mp}^2}{h_{\pm}^2} \right) \chi\omega_{10} - (3h_{\pm}^2 + h_{\mp}^2) \gamma\Omega_{10} \right] \\ \frac{1}{\sqrt{N}} \left\{ \mp \left[\frac{N-2h_{\mp}^2(3h_{\pm}^2 + h_{\mp}^2)}{h_{\pm}^2} \right] \chi\omega_{10} + [N-2h_{\mp}^2(3h_{\pm}^2 + h_{\mp}^2)] \gamma\Omega_{10} \right\} \end{pmatrix}, \quad (72)$$

and

$$\begin{pmatrix} \langle 1_0 1_{B(k)} | \\ \langle 1_{B(k)}^2 | \\ \langle 2_{B(k)} | \end{pmatrix} |2_{DB(k)}\rangle^{(1)} = \frac{\sqrt{2(N-2)}}{h_+ h_- N\Omega_{10}} \begin{pmatrix} \chi\omega_{10} \\ -\sqrt{\frac{N-2}{N}} \left(\frac{h_+^2 - h_-^2}{h_+ h_-} \chi\omega_{10} + h_+ h_- \gamma\Omega_{10} \right) \\ -\sqrt{\frac{2}{N}} \left(\frac{h_+^2 - h_-^2}{h_+ h_-} \chi\omega_{10} + h_+ h_- \gamma\Omega_{10} \right) \end{pmatrix}. \quad (73)$$

The main lesson from these perturbative correction calculations is that the anharmonicity-induced energy shifts should be undetectable as they scale as $1/N \rightarrow 0$ when $N \gg 1$, as is the case of collective SC. Hence, calculations using one or small number of emitters cannot accurately model the non-linear response of vibrational polariton systems under those conditions.

IV. CONCLUSIONS

In this work, we have found the exact eigenspectrum of the doubly excited manifold of an ensemble of N anharmonic oscillators under collective VSC. We provided a group-theoretical formalism to solve this many-body problem, reducing it to small matrix diagonalizations (the largest of which involves a 4×4 matrix). This procedure is a significant simplification from the brute-force numerical approach,

TABLE II. Eigenfrequencies in the doubly excited manifold. The Tavis-Cummings (TC) model is effectively an anharmonic system with $\chi = 0$ and $\gamma = -1$; therefore, when $N \gg 1$, the TC model yields the same results as the Harmonic limit.

Eigenmode	Harmonic limit	$O(\chi, \gamma)$ anharmonic corrections
2_{\pm}	$2\omega_{\pm}$	$-\frac{h_{\pm}^4}{N} (\chi\omega_{10} \mp 4h_{\pm}^2\gamma\Omega_{10})$
1_+1_-	$\omega_0 + \omega_{10}$	$-\frac{2h_+^2h_-^2}{N} [(1 - \delta_{h_+h_-})\chi\omega_{10} - 2(h_+^2 - h_-^2)\gamma\Omega_{10}]$
2_{DA}	$2\omega_{10}$	$-\frac{2N-2 + \delta_{h_+h_-}}{2N} \chi\omega_{10}$
$1_{\pm}1_B$	$\omega_{10} + \omega_{\pm}$	$-\frac{2h_{\pm}^2}{N} (\chi\omega_{10} \mp 2h_{\pm}^2\gamma\Omega_{10})$
2_{DB}	$2\omega_{10}$	$-\frac{N-2}{N} \chi\omega_{10}$
1_C^2	$2\omega_{10}$	0

TABLE III. Dipolar transition intensities between eigenstates carrying the totally symmetric irrep in the first and second excited manifolds.

$ \Psi\rangle$	$\langle\Psi \hat{\mu}/\mu_{10} \Phi\rangle$	
	$ 1_+\rangle$	$ 1_-\rangle$
Tavis-Cummings		
$ 2_+\rangle$	$\sqrt{2}h_-(h_+^2\sqrt{N} + h_-^2\sqrt{N-1})$	$\sqrt{2}h_+h_-^2(\sqrt{N-1} - \sqrt{N})$
$ 2_-\rangle$	$\sqrt{2}h_+h_-(\sqrt{N-1} - \sqrt{N})$	$\sqrt{2}h_+(h_+^2\sqrt{N-1} + \sqrt{2}h_-^2)$
$ 1_+1_-\rangle$	$h_+[h_+^2\sqrt{N} + h_-^2(2\sqrt{N-1} - \sqrt{N})]$	$h_-[h_+^2(2\sqrt{N-1} - \sqrt{N}) + h_-^2\sqrt{N}]$
Harmonic approximation		
$ 2_+\rangle$	$\sqrt{2N}h_-$	0
$ 2_-\rangle$	0	$\sqrt{2N}h_+$
$ 1_+1_-\rangle$	$\sqrt{N}h_+$	$\sqrt{N}h_-$
$ 2_{DA}\rangle$	0	0
$O(\chi, \gamma)$ anharmonic corrections		
$ 2_+\rangle$	$\sqrt{\frac{2}{N}}h_+^2h_-^3 \left[-\frac{\chi\omega_{10}}{\Omega_{10}} + (3h_+ - h_-^2)\gamma \right]$	$-\frac{h_+h_-^2}{\sqrt{2N}} \left[(h_+^2 + 2h_-^2) \frac{\chi\omega_{10}}{\Omega_{10}} - 2(h_+^2 - h_-^2 - 2h_+^2h_-^2)\gamma \right]$
$ 2_-\rangle$	$-\frac{h_+^2h_-}{\sqrt{2N}} \left[(2h_+^2 + h_-^2) \frac{\chi\omega_{10}}{\Omega_{10}} - 2(h_+^2 - h_-^2 - 2h_+^2h_-^2)\gamma \right]$	$\sqrt{\frac{2}{N}}h_+^3h_-^2 \left[\frac{\chi\omega_{10}}{\Omega_{10}} - (h_+ - 3h_-^2)\gamma \right]$
$ 1_+1_-\rangle$	$\frac{2h_+h_-^4}{\sqrt{N}} \left[\frac{\chi\omega_{10}}{\Omega_{10}} - (3h_+^2 - h_-^2)\gamma \right]$	$\frac{2h_+^4h_-}{\sqrt{N}} \left[-\frac{\chi\omega_{10}}{\Omega_{10}} + (h_+^2 - 3h_-^2)\gamma \right]$
	$\Delta \neq 0$	$-\sqrt{\frac{N(N-1)}{2N-1}}$
	$\Delta = 0$	$-\sqrt{\frac{N(N-1)}{2N-1}}$
$ 2_{DA}\rangle$	$\frac{\sqrt{N-1}}{2N} h_- \left[\frac{2h_+^2 - h_-^2}{h_+^2(h_+^2 - h_-^2)} \frac{\chi\omega_{10}}{\Omega_{10}} - 2\gamma \right]$	$\sqrt{\frac{N-1}{2N}} h_+ \left[-\frac{h_+^2 - 2h_-^2}{h_-^2(h_+^2 - h_-^2)} \frac{\chi\omega_{10}}{\Omega_{10}} - 2\gamma \right]$
	$\Delta \neq 0$	$\sqrt{\frac{N}{2(2N-1)}} - \frac{1}{2} \sqrt{\frac{2N-1}{2N}} \left(\frac{\chi\omega_{10}}{\Omega_{10}} + \gamma \right)$
	$\Delta = 0$	$\sqrt{\frac{N}{2(2N-1)}} - \frac{1}{2} \sqrt{\frac{2N-1}{2N}} \left(\frac{\chi\omega_{10}}{\Omega_{10}} + \gamma \right)$

which involves diagonalization of astronomically large $\binom{N+2}{2}$ -dimensional matrices where $N = 10^6 - 10^{10}$. We provide compact expressions and tables that should serve as a concise reference for future work involving the nonlinear spectroscopy of molecular polariton systems.

Through numerically exact examples and analytical studies using perturbation theory, we have contrasted this model to the standard TC and HO models, and have shown that the additionally available anharmonic transitions per molecule can give rise to new phenomena, such as enhancement of two-photon absorption cross-sections owing to new resonances

between bipolariton states and anharmonic two-quanta vibrational states. We have demonstrated that there are at most two such bipolariton states that fulfill those resonant conditions. These conclusions, while studied specifically for vibrational SC conditions, should have analogues in other frequency ranges, such as in the UV-visible regime, where anharmonic shifts in electronic transitions are ubiquitous.

We have provided with a summary of analytical expressions for eigenfrequencies and matrix elements of typical transition operators. These might serve as a reference guide for future theoretical and experimental explorations of the doubly ex-

TABLE IV. Dipolar transition intensities between eigenstates carrying the standard irrep in the first and second excited manifolds.

Model	$\langle 1_{\pm} 1_B \hat{\mu} / \mu_{10} 1_B \rangle$	$\langle 2_{DB} \hat{\mu} / \mu_{10} 1_B \rangle$
Tavis-Cummings Harmonic approximation	$h_{\mp} \sqrt{N-2}$ \sqrt{N}	- 0
$O(\chi, \gamma)$ anharmonic corrections	$\mp \frac{2h_{\pm} h_{\mp}}{\sqrt{N}} \left[\frac{\chi \omega_{10}}{\Omega_{10}} - (h_{\pm}^2 - h_{\mp}^2) \gamma \right]$	$-\sqrt{\frac{2(N-2)}{N}} \left(\frac{h_{\pm}^2 - h_{\mp}^2}{h_{\pm}^2 h_{\mp}^2} \frac{\chi \omega_{10}}{\Omega_{10}} + \gamma \right)$

TABLE V. Photon-induced transition intensities between eigenstates carrying the totally-symmetric irrep in the first and second excited manifolds.

$ \Psi\rangle$	$\langle \Psi \hat{a}_0 \Phi \rangle$	
	$ 1_{+}\rangle$	$ 1_{-}\rangle$
Tavis-Cummings		
$ 2_{+}\rangle$	$\sqrt{2}h_{+}$	0
$ 2_{-}\rangle$	0	$-\sqrt{2}h_{-}$
$ 1_{+}1_{-}\rangle$	$-h_{-}$	h_{+}
Harmonic approximation		
$ 2_{+}\rangle$	$\sqrt{2}h_{+}$	0
$ 2_{-}\rangle$	0	$-\sqrt{2}h_{-}$
$ 1_{+}1_{-}\rangle$	$-h_{-}$	h_{+}
$ 2_{DA}\rangle$	0	0
$O(\chi, \gamma)$ anharmonic corrections		
$ 2_{+}\rangle$	$\frac{\sqrt{2}h_{+}h_{+}^2}{N} \left[\frac{\chi \omega_{10}}{\Omega_{10}} - (3h_{+} - h_{-}^2) \gamma \right]$	$\frac{h_{+}^2 h_{-}^3}{\sqrt{2}N} \left(-\frac{\chi \omega_{10}}{\Omega_{10}} + 4h_{+}^2 \gamma \right)$
$ 2_{-}\rangle$	$-\frac{h_{-}^3 h_{-}^2}{\sqrt{2}N} \left(\frac{\chi \omega_{10}}{\Omega_{10}} + 4h_{-}^2 \gamma \right)$	$\frac{\sqrt{2}h_{+}^4 h_{-}}{N} \left[\frac{\chi \omega_{10}}{\Omega_{10}} - (h_{+} - 3h_{-}^2) \gamma \right]$
$ 1_{+}1_{-}\rangle$	$\frac{2h_{+}^2 h_{-}^3}{N} \left[\frac{\chi \omega_{10}}{\Omega_{10}} - (3h_{+}^2 - h_{-}^2) \gamma \right]$	$\frac{2h_{+}^3 h_{-}^2}{N} \left[\frac{\chi \omega_{10}}{\Omega_{10}} - (h_{+}^2 - 3h_{-}^2) \gamma \right]$
	$\Delta \neq 0$	
	$\Delta = 0$	$-\sqrt{\frac{N-1}{2N-1}}$
$ 2_{DA}\rangle$	$\Delta \neq 0$	$\frac{1}{N} \sqrt{\frac{N-1}{2}} \frac{h_{+}^2}{h_{-} (h_{+}^2 - h_{-}^2)} \frac{\chi \omega_{10}}{\Omega_{10}}$
	$\Delta = 0$	$-\frac{1}{\sqrt{2(2N-1)}} + \frac{1}{2N} \sqrt{\frac{2N-1}{2}} \left(\frac{\chi \omega_{10}}{\Omega_{10}} - \gamma \right)$
		$\frac{1}{\sqrt{2(2N-1)}} + \frac{1}{2N} \sqrt{\frac{2N-1}{2}} \left(\frac{\chi \omega_{10}}{\Omega_{10}} + \gamma \right)$

cited manifold. We highlight the finding that the deviation from the harmonic behavior is negligible for large N . This statement seems to contradict reports of strong optical nonlinearities in systems under collective SC.^{39,68} The resolution to this apparent conundrum lies in recognizing the essential role of anharmonic dissipative processes in the creation of reservoirs populated with dark states.⁴⁴ This effect is not considered in the present formalism as it ignores dissipation, and focuses on the regime where multiphoton absorption processes occur faster than relaxation into dark states.

Finally, our work also shows that calculations involving few emitters and higher excitation manifolds (i.e. nonlinear response calculations) cannot provide a satisfactory approximation to the nonlinear optics of the collective SC regime even if the single-molecule dipole is artificially increased to keep the overall light-matter coupling constant. We hope that these findings inform future experimental endeavors and the theoretical considerations regarding polaritonic chemical behavior and non-linear response.

Appendix A: Exact expressions for TC solutions.

Diagonalization of the TC Hamiltonian carrying the totally-symmetric irrep, eq. (41), entails solving a cubic characteristic polynomial. Although it is possible to obtain analytical expressions, this task is rather complicated and a numerical approach can be easily implemented if exact solutions are needed. Nonetheless, we list the eigenfrequencies for the corresponding bipolaritons as a reference:

$$\langle \Psi | \hat{H}_2 | \Psi \rangle_{\text{TC}} = \omega_0 + \omega_{10} + f_{\Psi}(\rho) \Omega_{10}, \quad (\text{A1})$$

where

$$f_{2+}(\rho) = 2\rho', \quad (\text{A2a})$$

$$f_{2-}(\rho) = -\rho' - \sqrt{3}\rho'', \quad (\text{A2b})$$

and

$$f_{1+1-}(\rho) = -\rho' + \sqrt{3}\rho''. \quad (\text{A2c})$$

In eq. (A2), ρ' and ρ'' refer to the real and imaginary parts, respectively, of the quantity ρ , which fulfills

$$\rho^3 = q^3 + i\sqrt{p^6 - q^6}, \quad (\text{A3a})$$

TABLE VI. Photon-induced transition intensities between eigenstates carrying the standard irrep in the first and second excited manifolds.

Model	$\langle 1_{\pm} 1_B \hat{a}_0 1_B \rangle$	$\langle 2_{DB} \hat{a}_0 1_B \rangle$
Tavis-Cummings	$\pm h_{\pm}$	-
Harmonic approximation	$\pm h_{\pm}$	0
$O(\chi, \gamma)$ anharmonic corrections	$\mp \frac{2h_+ h_+ h_-}{\sqrt{N}} \left[\frac{\chi \omega_{10}}{\Omega_{10}} - (h_+^2 - h_-^2) \gamma \right]$	$-\sqrt{\frac{2(N-2)}{N}} \left(\frac{h_+^2 - h_-^2}{h_+^2 h_-^2} \frac{\chi \omega_{10}}{\Omega_{10}} + \gamma \right)$

where the coefficients p and q are such that

$$p^2 = \frac{N - 2h_+^2 h_-^2}{3N} = \frac{1}{3} \left(1 - \frac{2g_{10}^2}{\Omega_{10}^2} \right), \quad (\text{A3b})$$

and

$$q^3 = \frac{h_+^2 h_-^2}{N} (h_+^2 - h_-^2) = \frac{g_{10}^2}{\Omega_{10}^3} \Delta. \quad (\text{A3c})$$

Finally, the eigenvectors are given by

$$|\Psi\rangle = \mathcal{N}_{\Psi} \begin{pmatrix} 2\sqrt{N-1} h_+^2 h_-^2 \\ \sqrt{2(N-1)} h_+ h_- \varphi_{\Psi}(\rho) \\ \sqrt{N} (f_{\Psi}(\rho) \varphi_{\Psi}(\rho) - 2h_+^2 h_-^2) \end{pmatrix}, \quad (\text{A4})$$

where $\varphi_{\Psi}(\rho) = f_{\Psi}(\rho) - h_+^2 + h_-^2$, and \mathcal{N}_{Ψ} is a normalization coefficient.

Appendix B: Fourier basis with two excitations.

In this section, we discuss the dark states that emerge in the doubly excited manifold beyond of what was covered on the main body of the manuscript. In the harmonic limit, a transparent way to generate dark states with meaningful labels is through the application of two creation operators related to the eigenmodes. Explicitly, these states are

$$|2_{\gamma D(k)}\rangle = \frac{\hat{a}_{B(k)}^{\dagger}}{\sqrt{2}} |1_{B(k)}\rangle, \quad (\text{B1a})$$

and

$$|1_{\gamma D(k\ell)}^2\rangle = \hat{a}_{B(k)}^{\dagger} |1_{B(\ell)}\rangle = \hat{a}_{B(\ell)}^{\dagger} |1_{B(k)}\rangle. \quad (\text{B1b})$$

The labels k and ℓ clearly indicate either the emitters in which the wavefunction is mostly localized, if the Schur-Weyl basis

is used, or the wave numbers assigned to the eigenfunction, in the case of the Fourier basis. However, these functions no longer carry a defined irrep, but instead the $N(N-1)/2$ -dimensional reducible representation $\gamma = A + B + C$ (not to be confused with the electric anharmonicity parameter).

The generation of states carrying the standard irrep has been presented in section III, as well as the explicit form of the C-symmetric states in the Schur-Weyl basis, where

$$\alpha_{mn}^{(k\ell)} = \alpha_m^{(k)} \alpha_n^{(\ell)} + \alpha_n^{(k)} \alpha_m^{(\ell)} - 2 \left(\alpha_m^{(k)} \delta_{n\ell} + \alpha_n^{(k)} \delta_{m\ell} \right). \quad (\text{B2})$$

In the case of the Fourier basis, we illustrate the application of eq. (33) for a scenario with four emitters. After removing

TABLE VII. Coefficients of center of mass and relative wave number for wavefunctions with $N = 4$.

w	w'	K	q
0	0	0	0
0	1	1	1
0	2	2	2
0	3	3	3
1	1	2	0
1	2	3	1
1	3	4	2
2	2	4	0
2	3	5	1
3	3	6	0

the functions with symmetries A and B, for $N = 4$, we have $N(N-3)/2 = 2$, and it can be checked, with the Schur-Weyl basis, that the allowed values for k and ℓ are $\{2, 3\}$ and 4, respectively. For $N = 4$, we can define the wave vectors proportional to $0 \leq w \leq 3$. This fact gives rise to the combinations of center of mass, K , and relative wave number, q , shown in table VII.

Plugging these into eq. (33), we get

$$\begin{aligned} c_{mn}^{(k,4)} = & \psi(0,0) + \psi(2,0)e^{\frac{\pi i}{2}(m+n)} + \psi(4,0)e^{\pi i(m+n)} + \psi(6,0)e^{\frac{3\pi i}{2}(m+n)} \\ & + \left[\psi(1,1)e^{\frac{\pi i}{4}(m+n)} + \psi(3,1)e^{\frac{3\pi i}{4}(m+n)} + \psi(5,1)e^{\frac{5\pi i}{4}(m+n)} \right] \cos\left(\pi \frac{m-n}{4}\right) \\ & + \left[\psi(2,2)e^{\frac{\pi i}{2}(m+n)} + \psi(4,2)e^{\pi i(m+n)} \right] \cos\left(\pi \frac{m-n}{2}\right) + \psi(3,3)e^{\frac{3\pi i}{4}(m+n)} \cos\left(3\pi \frac{m-n}{4}\right). \quad (\text{B3}) \end{aligned}$$

With help of Gram-Schmidt orthogonalization, it is possi-

ble to conclude that all coefficients $\psi(K_{k,4}, q_{k,4})$ vanish, ex-

cept for $\psi(6,0)$, $\psi(4,0)$, $\psi(4,2)$, and $\psi(2,2)$. With this information, we can write write

$$c_{mn}^{(k,4)} = \frac{1}{2\sqrt{3}} e^{\pi i(m+n)} \left[\cos\left(\pi \frac{m-n}{2}\right) - 1 \right], \quad (\text{B4a})$$

and

$$c_{mn}^{(k',4)} = -\frac{1}{2} \left[e^{\frac{3\pi i}{2}(m+n)} + e^{\frac{\pi i}{2}(m+n)} \cos\left(\pi \frac{m-n}{2}\right) \right]. \quad (\text{B4b})$$

Identifying the appropriate values for k and k' is rather cumbersome and escapes the scope of this work.

ACKNOWLEDGMENTS

JACGA thanks Stephan van den Wildenberg and Matthew Du for their useful comments and insights. The authors acknowledge funding support from the Air Force Office of Scientific Research award FA9550-18-1-0289.

- ¹R. F. Ribeiro, L. A. Martínez-Martínez, M. Du, J. Campos-Gonzalez-Angulo, and J. Yuen-Zhou, *Chem. Sci.* **9**, 6325 (2018).
- ²J. Feist, J. Galego, and F. J. Garcia-Vidal, *ACS Photonics* **5**, 205 (2018).
- ³J. Flick, N. Rivera, and P. Narang, *Nanophotonics* **7**, 1479 (2018).
- ⁴J. Garcia-Vidal Francisco, C. Cristiano, and W. Ebbesen Thomas, *Science* **373**, eabd0336 (2021).
- ⁵D. N. Basov, A. Asenjo-Garcia, P. J. Schuck, X. Zhu, and A. Rubio, *Nanophotonics* **10**, 549 (2021).
- ⁶J. D. Plumhof, T. Stöferle, L. Mai, U. Scherf, and R. F. Mahrt, *Nature Materials* **13**, 247 (2014).
- ⁷J. Keeling and S. Kéna-Cohen, *Annu. Rev. Phys. Chem.* **71**, 435 (2020).
- ⁸M. A. Zeb, P. G. Kirton, and J. Keeling, arXiv preprint arXiv:2004.09790 (2020).
- ⁹S. Pannir-Sivajothi, J. A. Campos-Gonzalez-Angulo, L. A. Martínez-Martínez, S. Sinha, and J. Yuen-Zhou, arXiv preprint arXiv:2106.12156 (2021).
- ¹⁰K. Georgiou et al., *ACS Photonics* **5**, 258 (2018).
- ¹¹L. A. Martínez-Martínez, E. Eizner, S. Kéna-Cohen, and J. Yuen-Zhou, *The Journal of Chemical Physics* **151**, 054106 (2019).
- ¹²T. W. Ebbesen, *Acc. Chem. Res.* **49**, 2403 (2016).
- ¹³J. Yuen-Zhou and V. M. Menon, *Proceedings of the National Academy of Sciences* **116**, 5214 (2019).
- ¹⁴F. Herrera and J. Owrutsky, *J. Chem. Phys.* **152**, 100902 (2020).
- ¹⁵A. Blais, R.-S. Huang, A. Wallraff, S. M. Girvin, and R. J. Schoelkopf, *Phys. Rev. A* **69**, 062320 (2004).
- ¹⁶J. Peng et al., *Phys. Rev. Lett.* **127**, 043604 (2021).
- ¹⁷V. Agranovich, *Optika i Spektroskopiya* **3**, 84 (1957).
- ¹⁸J. J. Hopfield, *PR* **112**, 1555 (1958).
- ¹⁹C. Weisbuch, M. Nishioka, A. Ishikawa, and Y. Arakawa, *Phys. Rev. Lett.* **69**, 3314 (1992).
- ²⁰D. G. Lidzey et al., *Nature* **395**, 53 (1998).
- ²¹I. I. Rabi, *Phys. Rev.* **51**, 652 (1937).
- ²²E. T. Jaynes and F. W. Cummings, *Proceedings of the IEEE* **51**, 89 (1963).
- ²³R. H. Dicke, *Phys. Rev.* **93**, 99 (1954).
- ²⁴M. Tavis and F. W. Cummings, *Phys. Rev.* **170**, 379 (1968).
- ²⁵V. F. Crum, S. R. Casey, and J. R. Sparks, *Phys. Chem. Chem. Phys.* **20**, 850 (2018).
- ²⁶K. Hirai, J. A. Hutchison, and H. Uji-i, *ChemPlusChem* **85**, 1981 (2020).
- ²⁷J. D. Erwin, Y. Wang, R. C. Bradley, and J. V. Coe, *J. Phys. Chem. B* **125**, 8472 (2021).
- ²⁸A. B. Grafton et al., *Nature Communications* **12**, 214 (2021).
- ²⁹K. Nagarajan, A. Thomas, and T. W. Ebbesen, *J. Am. Chem. Soc.* **143**, 16877 (2021).
- ³⁰D. S. Wang and S. F. Yelin, *ACS Photonics* **8**, 2818 (2021).
- ³¹B. Xiang and W. Xiong, *The Journal of Chemical Physics* **155**, 050901 (2021).
- ³²J. Yuen-Zhou, J. A. Campos-González-Angulo, R. F. Ribeiro, and M. Du, *Vibropolaritonic chemistry: theoretical perspectives*, in *Metamaterials, Metadevices, and Metasystems 2021*, edited by N. Engheta, M. A. Noginov, and N. I. Zheludev, volume 11795, pages 6 – 17, International Society for Optics and Photonics, SPIE, 2021.
- ³³F. J. Hernández and F. Herrera, *The Journal of Chemical Physics* **151**, 144116 (2019).
- ³⁴J. F. Triana, F. J. Hernández, and F. Herrera, *The Journal of Chemical Physics* **152**, 234111 (2020).
- ³⁵E. W. Fischer and P. Saalfrank, *The Journal of Chemical Physics* **154**, 104311 (2021).
- ³⁶C. Schäfer, J. Flick, E. Ronca, P. Narang, and A. Rubio, arXiv preprint arXiv:2104.12429 (2021).
- ³⁷D. S. Wang, T. Neuman, S. F. Yelin, and J. Flick, arXiv preprint arXiv:2109.06631 (2021).
- ³⁸N. Takemura et al., *Phys. Rev. B* **92**, 125415 (2015).
- ³⁹B. Xiang et al., *Proceedings of the National Academy of Sciences* **115**, 4845 (2018).
- ⁴⁰B. Xiang et al., *J. Phys. Chem. A* **123**, 5918 (2019).
- ⁴¹T. M. Autry et al., *Phys. Rev. Lett.* **125**, 067403 (2020).
- ⁴²C. A. DelPo et al., *J. Phys. Chem. Lett.* **11**, 2667 (2020).
- ⁴³R. Duan, J. N. Mastron, Y. Song, and K. J. Kubarych, *J. Phys. Chem. Lett.* **12**, 11406 (2021).
- ⁴⁴R. F. Ribeiro et al., *J. Phys. Chem. Lett.* **9**, 3766 (2018).
- ⁴⁵P. Saurabh and S. Mukamel, *J. Chem. Phys.* **144**, 124115 (2018).
- ⁴⁶A. Debnath and A. Rubio, *Journal of Applied Physics* **128**, 113102 (2020).
- ⁴⁷B. Gu and S. Mukamel, *J. Phys. Chem. Lett.* **11**, 8177 (2020).
- ⁴⁸T. E. Li, A. Nitzan, and J. E. Subotnik, *The Journal of Chemical Physics* **154**, 094124 (2021).
- ⁴⁹R. F. Ribeiro, J. A. Campos-Gonzalez-Angulo, N. C. Giebink, W. Xiong, and J. Yuen-Zhou, *Phys. Rev. A* **103**, 063111 (2021).
- ⁵⁰F. T. Arecchi, E. Courtens, R. Gilmore, and H. Thomas, *Phys. Rev. A* **6**, 2211 (1972).
- ⁵¹R. Gilmore, *Ann. Phys.* **74**, 391 (1972).
- ⁵²M. Gegg and M. Richter, *New J. Phys.* **18**, 043037 (2016).
- ⁵³N. Shammah, S. Ahmed, N. Lambert, S. De Liberato, and F. Nori, *Phys. Rev. A* **98**, 063815 (2018).
- ⁵⁴Y.-H. Lee, J. Links, and Y.-Z. Zhang, *Nonlinearity* **24**, 1975 (2011).
- ⁵⁵T. Skrypnik, *J. Math. Phys.* **56**, 023511 (2015).
- ⁵⁶J. A. Campos-Gonzalez-Angulo, R. F. Ribeiro, and J. Yuen-Zhou, **23**, 063081 (2021).
- ⁵⁷M. A. Bastarrachea-Magnani, S. Lerma-Hernández, and J. G. Hirsch, *Phys. Rev. A* **89**, 032101 (2014).
- ⁵⁸E. Choreño, D. Ojeda-Guillén, and V. D. Granados, *Journal of Mathematical Physics* **59**, 073506 (2018).
- ⁵⁹A. Klimov and S. Chumakov, *A Group-Theoretical Approach to Quantum Optics: Models of Atom-Field Interactions*, Wiley, 2009.
- ⁶⁰A. Strashko and J. Keeling, *Phys Rev A* **94**, 023843 (2016).
- ⁶¹M. Scully and M. Zubairy, *Quantum Optics*, Cambridge University Press, 1997.
- ⁶²S. Cordero, O. Castaños, R. López-Peña, and E. Nahmad-Achar, *J. Phys. A: Math. Theor.* **46**, 505302 (2013).
- ⁶³A. Bohr and B. Mottelson, *Nuclear Structure (In 2 Volumes)*, World Scientific Publishing Company, 1998.
- ⁶⁴H. Lipkin, *Lie Groups for Pedestrians*, Dover Books on Physics Series, Dover Publications, 2002.
- ⁶⁵A. L. Ivanov and H. Haug, *Phys. Rev. Lett.* **74**, 438 (1995).
- ⁶⁶P. M. Morse, *Phys. Rev.* **34**, 57 (1929).
- ⁶⁷E. F. de Lima and J. E. M. Hornos, *J. Phys. B: At., Mol. Opt. Phys.* **38**, 815 (2005).
- ⁶⁸A. D. Dunkelberger, B. T. Spann, K. P. Fears, B. S. Simpkins, and J. C. Owrutsky, *Nature Communications* **7**, 13504 (2016).